

Host Galaxies of Gamma-Ray Bursts

Stéphanie Courty, Gunnlaugur Björnsson and Einar H. Guðmundsson

Raunvísindastofnun Háskólans

Vefútgáfa: 30. nóv. 2004

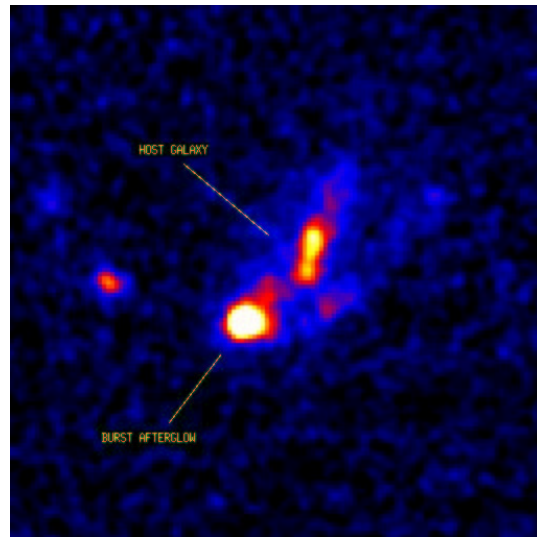
Abstract – Gamma-ray bursts (GRBs) are the most energetic events in the universe and can therefore be seen at large cosmological distances. According to present theoretical understanding, at least some of the bursts result from the core collapse and explosion of massive stars. Since massive stars are found in star forming regions, GRBs and by extension their host galaxies, are considered to be an important tool for understanding the formation and cosmological evolution of galaxies. The scenario of galaxy formation involves the basic idea that gravitating dark matter creates a network of overdense structures into which the baryonic matter is accreted and then cools to form stars and galaxies. Using numerical simulations able to reproduce such a scenario, we investigate the nature of GRB host galaxies and show that these are objects of rather low luminosity. As a result GRBs appear to be an efficient tool to trace galaxies which are otherwise difficult to detect.

1. Introduction

Gamma-ray bursts (GRBs) are short-lived bursts of gamma-ray photons. They appear at random from any direction on the sky, last from a few milliseconds to several minutes and can be hundreds of times brighter than a typical supernova. This makes them briefly the brightest sources in the observable Universe. GRBs longer than about few seconds are believed to result from the deaths of very massive stars typically occurring in galaxies currently in a phase of active star formation.

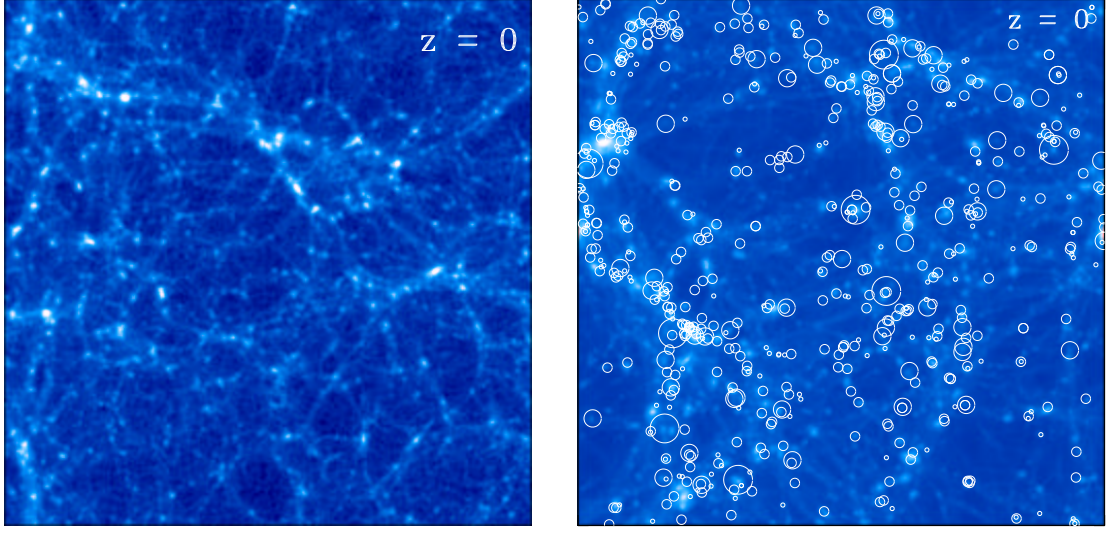
The spatial distribution of galaxies in the universe, their formation and their evolution are key issues in cosmology. Host galaxies of GRBs, an example of which is shown in Fig. 1, are considered to be a useful tracer of galaxy formation, since the association of GRBs with sites of star formation and their extreme brightness makes them observable to very high redshifts. They are therefore able to reveal high redshift galaxies that would be very difficult to detect otherwise.

The investigation of the host galaxy properties is therefore of fundamental importance and needs to be addressed. Although observational data is rather limited in number at present, it tends to show that hosts are compact, blue, low-luminosity galaxies. We ex-



Mynd 1. A section of the Hubble Space Telescope image of the field of GRB 990123, showing the optical afterglow and its host galaxy, taken about 16 days after the burst (The Caltech GRB Team/Space Telescope Science Institute) .

amine this association theoretically using a numerical approach. The simulations presented here are computed for a Λ –cold dark matter cosmological scenario



Mynd 2. Left: Projection of the entire computational volume of the dark matter density contrast at $z = 0$, the density scale spans from dark blue (lowest) to white (highest). Right: The same but with the projection of the spatial distribution of galaxies superimposed, each galaxy is shown by a circle with a radius proportional to its mass. Only 600 objects randomly chosen in the computational volume are plotted and the four increasing circle sizes represent objects with $M < 10^8$, $10^8 < M < 10^9$, $10^9 < M < 10^{11}$, $M > 10^{11} M_{\odot}$, respectively.

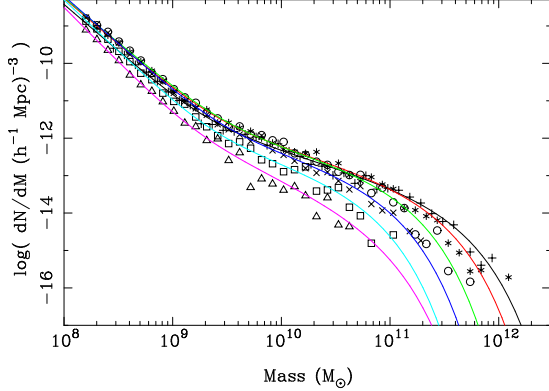
defined by: $H_0 = 70 \text{ km s}^{-1} \text{ Mpc}^{-1}$, $\Omega_K = 0$, $\Omega_m = 0.3$, $\Omega_{\Lambda} = 0.7$, $\Omega_b = 0.02h^{-2}$ with $h = H_0/100 \text{ km s}^{-1} \text{ Mpc}^{-1}$. The adopted resolution is as follows: The number of dark matter particles is 256^3 , as well as the number of grid cells; The comoving size of the computational volume is $L_{box} = 32 h^{-1} \text{ Mpc}$, giving a dark matter particle mass of $2.01 \times 10^8 M_{\odot}$, and a gas mass initially enclosed in each grid cell of $3.09 \times 10^7 M_{\odot}$. The simulations were performed on NEC-SX5 at the Institut du Développement et des Ressources en Informatique Scientifique (France).

2. Galaxy formation in numerical simulations

The main ideas involved in the hierarchical galaxy formation scenario are the following: At the very large scales of the universe a network of dark matter overdense structures is created by gravitational instability. Inside, baryonic matter is accreted, it cools and contracts to form stars and galaxies (Figure 2). Reproducing this scenario numerically requires following self-consistently the dynamical evolution of the dark matter as well as the dynamical evolution of the baryonic matter in an expanding universe. The non-collisional dark matter is sampled by particles, and the baryonic matter is discretized on a grid. Dynamical

equations are solved for both fluids in the Newtonian approximation, where the gravitational potential satisfies the Poisson equation which describes the coupling between gas and dark matter. The difference between the two sets of equations comes from the dissipative terms in the gas equations. Hydrodynamical shocks undergone by the gas accreted in the dark matter potential wells are treated with the artificial viscosity method and the code includes radiative cooling processes to simulate the concentration of the gas: collisional excitation, collisional ionization, recombination, bremsstrahlung and Compton scattering. No heating term is included, since our aim is to consider only the most dominant processes involved in galaxy formation. More details on the 3D N-body/Eulerian code can be found in [1].

Since the simulations do not have sufficient resolutions to resolve the complex process of star formation at scales smaller than the cell size, galaxy formation is described by a set of physically motivated prescriptions. The model consists of the identification of the gas regions satisfying the necessary conditions for a galaxy to form, one of the important criteria being that the cooling timescale must be less than the

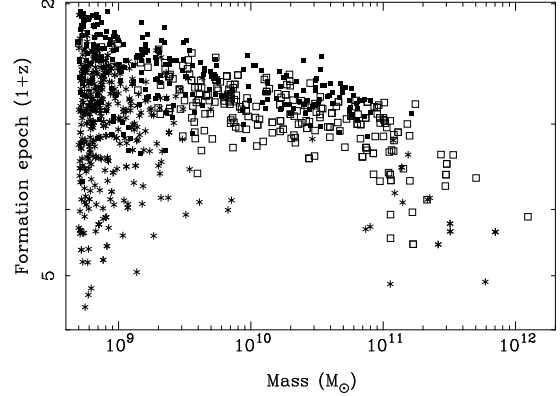


Mynd 3. Galaxy mass functions as revealed in the simulations from $z = 5$ to $z = 0$ (symbols, from bottom to top). The curves are the fits by two power-law Schechter functions.

dynamical timescale [2]. A fraction of the gas in the cells satisfying these conditions is turned into a “stellar particle”, each identified by its epoch of formation and its mass, where the latter ranges between 10^6 and a few $10^8 M_\odot$. The cosmological evolution of these particles is treated in a same way as the dark matter.

Galaxies are then defined by grouping the stellar particles at different redshifts. Fig. 2 is the projection of the dark matter density contrast at redshift $z = 0$, (today’s epoch, left panel), and superimposed on it is the projection of the galaxy distribution (right panel). Galaxies are represented by circles whose radii are proportional to the galaxy mass. The spatial distribution of galaxies on large scales follows the spatial distribution of the dark matter.

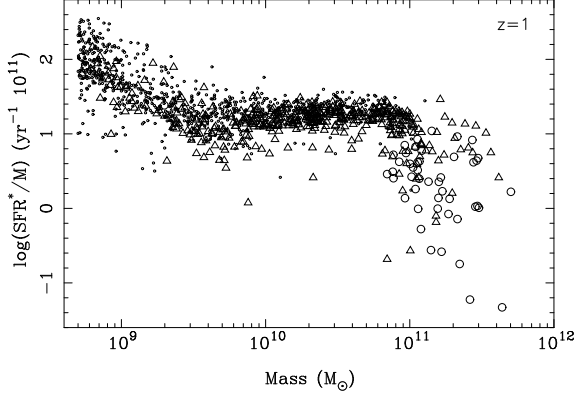
An important quantity for the theory of galaxy formation is the mass function, i.e. an estimate of the number of galaxies per interval of mass as a function of mass. Its observational counterpart is the luminosity function. It is usually fitted by a power-law Schechter function [3], combining an exponential at the bright end with a power-law at the faint end. Figure 3 presents the cosmological evolution of the galaxy mass function from $z = 5$ to $z = 0$ obtained in the simulations. The mass functions extend from $\sim 10^8$ to a few times $10^{12} M_\odot$ at low redshift and show a characteristic shape, similar to the galaxy luminosity function. The decrease at the high-mass end is clearly seen at low redshift, suggesting an evolution in redshift: the break between



Mynd 4. Epoch of formation of galaxies as a function of their mass at $z = 1$ (the higher the value, the older the galaxy). Stars refer to galaxies with $SFR^* = 0$. The star-forming population (with non-zero SFR^*) is divided according to the value of the efficiency parameter: $\epsilon > 1.3$ (filled squares) and $\epsilon < 1.3$ (empty squares).

the exponential behavior and the power-law is shifted towards higher mass as the redshift decreases: galaxies increase their mass as evolution proceeds, due to the merging processes between smaller galaxies and/or the accretion of new gas. However, the main feature of our numerical galaxy catalogs is that at any redshift the mass functions are dominated by a significant population of low-mass galaxies, $M < 5 \cdot 10^{10} M_\odot$. To take this population into account, we use a fit combining a standard Schechter function with a power-law at the very low-mass end. The parameters of the fit at low redshift are consistent with the parameters of the observed galaxy luminosity function determined from different surveys.

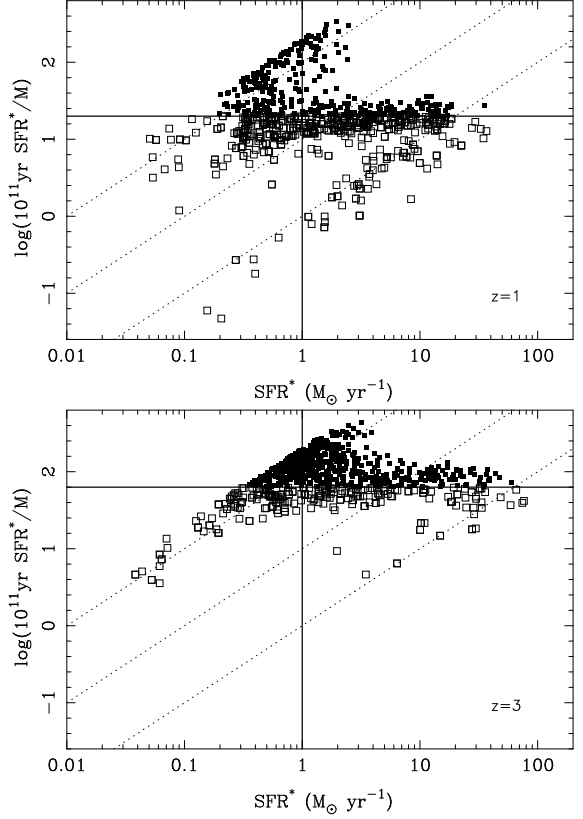
In addition to the mass, the simulated galaxies are characterized by an epoch of formation and an instantaneous star formation rate, denoted by SFR^* . The first quantity is the mean epoch of formation of all the stellar particles the galaxy is composed of, weighted by the mass of each particle. The second quantity estimates the amount of stellar mass produced over a period of 10^8 yr (before a given observational time). In Figure 4 we plot a diagram showing the epoch of formation versus mass and where we distinguish objects according to their SFR^* at $z = 1$. The simulated catalog of galaxies clearly shows distinct sub-populations. The high-mass population in Fig. 4 mainly includes old galaxies in which star formation has ceased. These



Mynd 5. Efficiency parameter, ϵ , versus mass for galaxies at $z = 1$. For clarity, only 1000 objects randomly chosen from the catalog are plotted. The symbols indicate the epoch of formation of each galaxy: less than $z = 1.8$ (dots), in the range $z = 1.8 - 2.4$ (triangles) and greater than $z = 2.4$ (open circles).

galaxies are located in the center of the biggest dark matter halos at low redshift. Indeed as evolution proceeds, dark matter potential wells become too deep for the accreting gas to cool and form stars, subsequently quenching the star formation activity in the high-mass galaxies. The galaxy population includes also a large number of low-mass galaxies formed at early epochs. On the other hand, the star-forming population includes intermediate and low-mass galaxies, some of them being quite young.

Since our model considers a galaxy formation dependent on the baryonic density contrast, and the star formation rate is roughly proportional to the galaxy mass, a large dispersion appears at low redshift for the high-mass galaxies. This dispersion can be seen in Figure 5, where we now show only the star-forming galaxies and where the ratio between the SFR^* and the mass is plotted against the galaxy mass. Note that high-mass galaxies may have SFR^* as low as low-mass galaxies, while the latter are much more efficient than high-mass galaxies in their star formation. Indeed, if the SFR^* quantifies the amount of gas converted into stellar matter, the ratio SFR^*/M measures how efficient this transformation is. The trend that the efficiency increases as the galaxy mass decreases is consistent with observations [4]. In the rest of this paper we describe this efficiency by the parameter ϵ derived

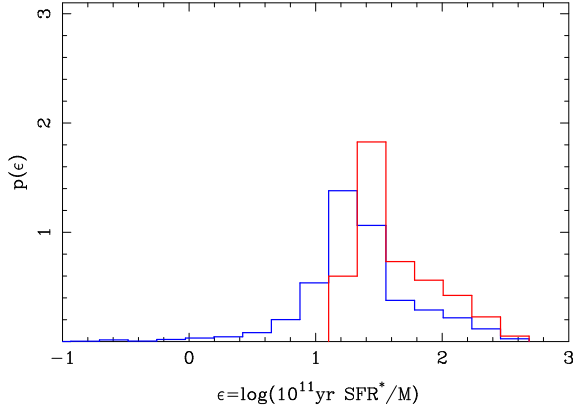


Mynd 6. Upper panel: Star-forming efficiency (specific star formation rate) versus activity (star formation rate) for host galaxies (filled squares) and non-host galaxies (empty squares) as defined in the catalog at $z = 1$. For clarity, only 1000 objects randomly chosen from the catalog are plotted. Diagonal lines are equal galaxy mass lines, 10^9 , 10^{10} , 10^{11} M_\odot (from left to right). Lower panel: Same, but for the catalog at $z = 3$.

from the specific star formation rate as:

$$\begin{aligned} \epsilon &\equiv \log \left(\frac{SFR^*}{M_\odot \text{yr}^{-1}} \right) \left(\frac{M}{10^{11} M_\odot} \right)^{-1} \\ &= \log(10^{11} \text{yr} SFR^*/M). \end{aligned} \quad (1)$$

Among the key issues in galaxy formation today is describing how different sub-populations of galaxies distinguish themselves and understanding the different processes involved in their evolution. These low-mass efficient galaxies are likely to be faint galaxies, especially at high redshift. Host galaxies of gamma-ray bursts could prove useful to shed light on the proper-



Mynd 7. Distributions of the efficiency parameter for the host galaxy population (red) compared to the overall galaxy population (blue), at $z = 1$. Each distribution is normalized on its total number of objects.

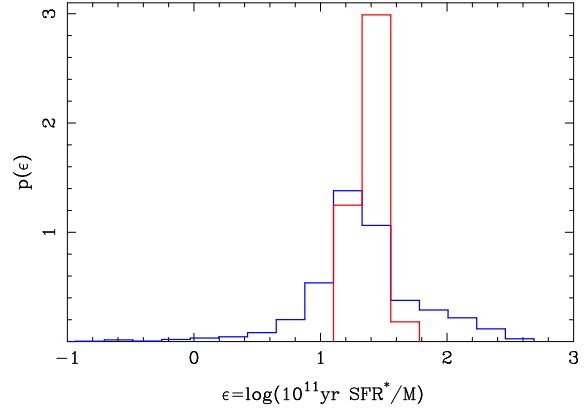
ties of these faintest galaxies. Indeed as mentioned in the introduction, a majority of GRBs appear to be in faint, blue galaxies.

3. Host galaxies

We can use our simulations to predict properties of host galaxies of GRBs. Since GRBs occur on scales outside the reach of our simulations, an assumption is required to select candidate host galaxies in the simulated catalogs. Based on the first observations of GRB hosts, we select host galaxies in the simulated catalogs as the most efficient star-forming objects, with $\epsilon > \bar{\epsilon}$, where $\bar{\epsilon}$ is an arbitrary threshold that depends on redshift, here chosen to be the average efficiency of the population. We then compare the host galaxy population with the overall population.

A powerful way to illustrate how the notions of star formation activity and star formation efficiency differ is to compare the SFR^* and ϵ . In the upper panel of Figure 6, the two symbols distinguish whether a galaxy is a host or not (with $\bar{\epsilon} = 1.3$ at $z = 1$). Diagonal lines are lines of equal galaxy mass. As before, different sub-populations are seen: for a given star formation rate the high-mass galaxies are much less efficient in their star formation than low-mass galaxies.

The majority of candidate host galaxies seem to be low-mass young objects with rather moderate SFR^* . This conclusion holds also at higher redshift (lower panel of Fig. 6), although the dispersion in the effi-



Mynd 8. Same as Fig. 7 but the low-mass galaxies are excluded from the host galaxy population.

ciency parameter is much more reduced. Note also that at a given mass the SFR^* increases with the redshift, and hence the efficiency parameter does so too. An interesting point is that a high-mass galaxy at $z = 3$ can have a similar efficiency parameter, for instance $\epsilon = 2$, as can a low-mass galaxy at $z = 1$. This result is consistent with [5], their single host at $z = 3$ has an SFR^*/M value close to the values for their six hosts at $z = 1$.

Figure 7 compares statistically the distributions of ϵ for the host galaxy population with the overall population. The two distributions are clearly different. Figure 8 shows the same comparison expect that now low-mass galaxies, with $M < 10^{10} M_{\odot}$, are excluded from the host population. The distribution for the hosts is peaked towards intermediate efficiency, and resembles the distribution obtained observationally [6]. The lack of faint galaxies in the observations suggests some bias. We would expect the host distribution to broaden as deeper observations become available.

Future observations are also expected to confirm whether or not the host galaxies populate the SFR^*/M - SFR^* diagram homogeneously. A negative confirmation could help to argue against a strong contribution of the hosts to the global star formation rate. For instance, the total star formation rate enclosed in our low-mass host galaxies amounts to less than 50% of the total star formation rate at $z = 1$. Concluding that the GRB formation rate does not follow the total SFR is not so unreasonable since the probability of forming a GRB from a high-mass star

is likely to depend on the environment and the history of the host galaxy: young galaxies with low-metallicity environment are more likely to form GRBs than evolved systems, although a few GRBs have been observed in such systems.

4. Conclusion

Selecting hosts as the most efficient galaxies in simulated catalogs allows us to interpret the first available observations, and to predict the cosmological evolution of host galaxies. A more detailed analysis can be found in [7]. The question then is: Why are the hosts likely to be efficient galaxies rather than galaxies with the highest SFR^* , for instance? The answer is likely to lie in the physics of the object itself (see [8] in this volume). These results are being used to explore the formation and evolution of galaxies at very high redshift. Future observations will confirm if hosts do not populate the $SFR^*/M-SFR^*$ diagram in an homogeneous way. If so, GRBs are not likely to trace the cosmic SFR, but nevertheless constitute a powerful tool to explore the faint end of the galaxy luminosity function.

Acknowledgments

The research reported in this paper was supported in part by a special grant from the Icelandic Research Council.

Samantekt: Í grein þessari er fjallað um tilraun til að nota viðamikla hermireikninga af myndun stórsærra efniseininga í alheimi til að varpa ljósi á eiginleika hýsilvetrarbrauta gammablossa. Hýslarnir eru flestir mjög daufir og hefðu að líkindum aldrei fundist ef blossaatburður hefði ekki orðið í þeim. Með hliðsjón af mælingum gerum við ráð fyrir að hýslarnir séu vetrarbrautir með háa eiginstjörnumyndun. Afleiðingar þessa á tölfraðilega eiginleika hýslanna sem safns eru skoðaðir og bornir saman við safnið sem fæst ef gert er ráð fyrir að hýslarnir séu vetrarbrautir með kröftuga stjörnumyndun. Mikilvægt er að skilja hvers vegna blossar hafa tilhneigingu til að verða frekar í vetrarbrautum með háa eiginstjörnumyndun fremur en háa stjörnumyndun. Svarið við því er að líkindum að miklu leiti háð eiginleikum stjörnunnar sem myndar atburðinn, en einnig eiginleikum vetrabrautarinnar sem blossin verður í. Ljóst er því að aukinn skilningur á eiginleikum hýsilvetrarbrauta mun í framtíðinni geta varpað mikilvægu ljósi á myndun og þessarra stærstu efniseininga í alheimi.

References

- [1] Teyssier, R., Chièze, J.-P., Alimi, J.-M., 1998, ApJ 509, 62
- [2] Rees, M. J. & Ostriker, J. P., 1977, MNRAS, 179, 541
- [3] Schechter, P., 1976, ApJ 203, 297
- [4] Guzman, R., Gallego, J., Koo, D. C., Phillips, A. C., Lowenthal, J. D., Faber, S. M., Illingworth, G. D., Vogt, N. P., 1997, ApJ 489, 559
- [5] Chary R., Becklin, E. E., Armus, L., 2002, ApJ 566, 229
- [6] Christensen, L., Hjorth, J., Gorosabel, J., 2004, A&A, 425, 913
- [7] Courty, S., Björnsson, G., Guðmundsson, E. H., 2004, MNRAS 354, 581
- [8] Guðlaugur Jóhannesson, Gunnlaugur Björnsson, Einar H. Guðmundsson, 2004, *Tímarit um raunvísindi og stærðfræði*, p. x-y

About the authors: Stéphanie Courty is a research scientist at the Science Institute, Gunnlaugur Björnsson is a research professor at the Science Institute, Einar H. Guðmundsson is a professor of physics at the University of Iceland

Science Institute
University of Iceland
Dunhaga 3, IS-107 Reykjavík
courty, gulli, einar@raunvis.hi.is
Móttekin 15. sept. 2004